

## Bifurcation of vortex dipole in the viscous incompressible flow around an airfoil

M. N. ZAKHARENKOV (ZHUKOVSKY)

THE VISCOUS incompressible flow around a NACA0012 airfoil at angle of attack equal to  $5^\circ$  and Reynolds numbers ( $Re$ ) of 5 000, 10 000, and 30 000 is considered. The Navier-Stokes equations written in terms of stream function and vorticity are solved by a finite-difference predictor-corrector algorithm. Distinctive feature of the algorithm is the strict fulfilment of pressure uniqueness condition in the stream. Special attention is paid to displaying the dispersion properties in the computed viscous flow. Development of the flow separation on the airfoil, surface vorticity waves (streaming waves) which intensify in the separation region and, especially, at the trailing edge (TE), leads to strong vortex-pressure (acoustic) transition in vicinity of TE, to generation of vortex spots and to bifurcation of vortex dipole at the leading (LE) and TE. The complex vortex disturbances are perturbed which partly are emitted from LE into upstreamflow, and partly merge into velocity-pressure disturbances and surface vorticity waves. Found are the physical grounds for inevitable development of dispersion in the vorticity fields at  $Re > 10\,000$ . The vortex dipole bifurcation is clearly defined as the main reason for dispersion impulse formation.

### 1. Introduction

THE VISCOUS INCOMPRESSIBLE flow around an airfoil at low and moderate Reynolds numbers was studied by many authors using different numerical algorithms, see [1 - 6] for example. The Reynolds number ( $Re$ ) of 10 000 is almost the limiting value for available solvers of complete Navier-Stokes equations. One must note that the essential differences in various authors' results obtained for  $Re = 10\,000$   $\alpha = 5^\circ$  (the reliability of every one is assumed and does not rise any doubts) show that we really have a strong dependence of solution on some physical factors which manifest themselves in different properties of the computed viscous flows. For this reason the aim of the paper is not only to assess the accuracy of presented results but to depict essential physical processes which influence essentially the "boundary" problems for the flows under study (laminar-turbulent transition). Such approach allows us to exclude the deterioration of computational study of viscous incompressible flow at Reynolds numbers characterized by basic variation of flow properties which are revealed in practice.

The case with  $Re = 10\,000$  and angle of attack equal to  $5^\circ$  for NACA0012 and Joukowski airfoils is presented in the works of four authors: GHIA *et al.* [1, 2], WU *et al.* [4], CHOI (referred to in [5]) and ZAKHARENKOV [3, 7, 8]. These results present three different solutions.

i) Results of Ghia show two different forms of streamline behaviour in the region of trailing edge (TE) for  $Re = 1000$ . Their difference is related to the angle of TE (for a finite angle and cusp). Time-history of the flow is not shown and flows are presented as two different steady flows. The values of  $C_x$  (drag) and  $C_y$  (lift) coefficients for  $Re = 1000$  do not coincide with unpublished results of Zakharenkov (however, the Ghia's pressure distribution can be reconstructed). The flow at  $Re = 10000$  is essentially unsteady, with strong separation being at the airfoil leeward side.

ii) Results of Zakharenkov for  $Re = 10000$  (and unpublished results for  $Re = 1000$ ) show that the flow around NACA0012 airfoil TE is unsteady. This flow is similar to Ghia's results for  $Re = 1000$  and, what is essential, reveal that both types of TE flow obtained by Ghia are really united in the unsteady streamline behavior. There is no strong dispersion in the flow at  $Re = 10000$  (in contrast with Ghia's results).

iii) Results of WU *et al.* for  $Re = 10000$  give the coincidence with results of Zakharenkov for  $C_y = 0.49$  (for circulation of velocity around an airfoil equal to  $-0.21$ ). But WU do not show the dependence of lift upon the velocity circulation. This dependence presents the non-classic law as Zakharenkov has shown in [3].

iv) Results of Choi reveal the Kármán vortex street in the wake. It is obvious that such flow possesses essentially different acoustic properties considered in [5]. The vortex spots discussed in [9, 10] present a more sophisticated acoustic field.

v) GHIA in [2] finds the attractor in the solution; in [9], Zakharenkov investigates soliton-like properties of the flow; these are two different problems.

Such differences of results and goals of many authors make it difficult to compare the accuracy of the obtained results because the main properties of computational codes and meshes are quite different. New investigations are necessary to reveal the reasons for such differences in solutions. One of the problems is the dispersion of vorticity fields in CFD solution.

In GHIA *et al.* [1] the solution for  $Re = 10000$  and angle of attack  $\alpha = 5^\circ$  is presented. Much attention is paid to both specific properties of finite-difference approximation on the C type computational mesh and setting the vorticity boundary condition for this mesh. Nevertheless, the numerical solution (illustrated in [1] by equal vorticity lines) displays essential dispersion of vorticity which is often categorized as computational errors. Such type of dispersion and dissipation of vorticity is characteristic of vortical flows simulated by finite-difference schemes whose (first) differential approximation (FDA) essentially depends on the coefficients at third- and fourth-order derivatives of vorticity (the first two terms of approximation residual), see [11–13]. Nevertheless the main feature of the flow at  $Re = 10000$  consists in there being fundamental reasons for vorticity dispersion and energy dissipation; these reasons are connected with vortex dipole bifurca-

tion. The vortex dipoles characterize the integral properties of vortex fields in the airfoil boundary flow for this value of  $Re$  (see [3, 7]), and are unstable under perturbation induced by trailing edge flow separation. The "dipole bifurcation" notion was introduced by SADOVSKY and TAGANOV in [14] for inviscid flow, but the coincidence of behavior of streamlines illustrated in [14] with streamlines obtained numerically in [3, 7, 15] allows us to adjoin this notion to the viscous flow. The physical phenomena in a viscous flow underline the sustained vortex dipole bifurcation.

The notion of "dipole bifurcation" corresponds to the phenomenon when the intensity of dipole in the flow (in a present case the dipole is related to a vorticity field in a boundary layer, see [9]) varies in time. As SADOVSKY and TAGANOV showed in [14], this variation leads to generation of vortex patterns. The period of vortex pattern generation depends on a number of factors but the process as a whole may be assessed in analogy with flow bifurcation known from the flow instability theory. Essentially, the dispersion properties of numerical solutions presented in this paper are mostly related to perturbations of vorticity field. The comparison with results of papers [12, 13] allows us to assess this perturbation with dispersion terms of F.D.A. for vorticity transport equation. For this reason we can say about the vorticity dispersion defined by specific terms of F.D.A. This selection is a major precondition for formulating more complex rheological laws characterizing this flow. These are the reasons defining the employment of the notions "vorticity dispersion", "dispersion impulse", and "vortex dipole bifurcation".

As we shall see later, the dipole bifurcation process in a viscous flow is associated with dispersion. For this reason, the solution presented in [1] can be regarded as a pioneering result which may be recommended for estimating the possibility to describe laminar-turbulent transition provoked by dispersion. This is a rather novel approach in comparison with the traditional direct simulation of transition due to wave - packet instability. It must be mentioned that GHIA *et al.* [1] consider their results as the laminar unsteady flow only.

The recent numeric results obtained in [16, 17] for Reynolds number from 1 000 to 100 000 show that many new physical phenomena are inherent in viscous incompressible flow around an airfoil. Examples include vortex lock-up of vorticity layers [16]; bursting of vortex layers, [16]; microdipole instability of vortex layer [7, 12], etc. Also, there exists the unique situation (in [16]): vortical boundary layer (BL) at  $Re = 10\,000$ , does perform nonequilibrium transition to the laminar sublayer in BL at  $Re = 100\,000$ . The generation and instability of critical layers considered in [18, 19] must also be mentioned as the major processes determining the effectiveness of numeric simulation of layered media. Heat transfer and dependence of viscosity on temperature are the physical factors which can play a crucial role in nonequilibrium transition of vortical layer which forms the boundary layer at  $Re = 10\,000$  into the laminar sublayer at  $Re = 100\,000$ .

When vortex structure of BL transforms from a two-layer pattern (with windward and leeward vorticity layers) to a multi-layer pattern at  $Re > 100\,000$ , we observe generation of vortex spots discussed in [9, 10] which are intermediate between vortex waves and the vortices themselves [10]. RYZHOV *et al.* showed in [20], that the moving vortex spots perturb the BL momentum thickness (momentum losses), and this perturbation participating in nonlinear process becomes a soliton. Thus a vortex spot reveals wave-specific properties in integral estimation of flow momentum itself (inherent in a vortex spot), see [20]. As a rule, the equations describing solitons and vortex spots contain dispersion and energy dissipation terms.

We have some examples [12, 13] that the dispersion and energy dissipation define the complex phenomena of large vortex destruction and explain the possible physical mechanism of vorticity imbalance in the temperature spots. For this reason it is natural to suppose that these processes (dispersion and energy dissipation) are the decisive factors in the formation, development and destruction of the spots possessing different physical/mechanical characteristics, i.e. temperature, momentum, turbulence spots.

The phenomena mentioned above demand a profound study before we can assess the critical values of dispersion/dissipation coefficients at FDA terms (which can be interpreted as new terms of Navier-Stokes equations employing a more complex rheological law than the Stokes law [13, 21]). Simultaneously the special property of computational model of viscous flow (to simulate the dispersion and energy dissipation properties) gives us the simple tool to study the dipole bifurcation by directly controlled computational simulation.

## 2. Problem statement and computational algorithm

The two-dimensional flow around an airfoil NACA0012 is studied by computational simulation based on the solution of Navier-Stokes equations written in the terms of stream function  $\Psi$  and vorticity  $\Omega$ . These functions are defined by relations

$$(2.1) \quad u = \frac{\partial \Psi}{\partial y}, \quad v = -\frac{\partial \Psi}{\partial x}, \quad \Omega = \frac{\partial u}{\partial y} - \frac{\partial v}{\partial x},$$

where  $u$  and  $v$  are velocity components in the  $\{x, y\}$  coordinates. Then the continuity condition is met through introduction of a stream function, and relations (2.1) led to the Poisson equation

$$(2.2) \quad \Delta \Psi = \Omega,$$

where  $\Delta$  is the Laplace operator. The momentum equations are transformed to

the vorticity transport equation (i.e., equation of vortex dynamics)

$$(2.3) \quad \frac{\partial \Omega}{\partial t} + u \frac{\partial \Omega}{\partial x} + v \frac{\partial \Omega}{\partial y} = \frac{1}{\text{Re}} \Delta \Omega,$$

where  $\text{Re} = U_\infty c / \nu$  is the Reynolds number,  $U_\infty$  the velocity of undisturbed flow,  $c$  is the airfoil chord, and  $\nu$  the coefficient of kinematic viscosity.

The no-slip condition on the airfoil surface  $s$ , the conditions of uniform flow (the asymptotics of far - field velocity and vorticity) on the outer boundary  $s_\infty$  of the computational domain, the initial conditions of rest (for the fluid and airfoil) complete the problem statement. The pressure is calculated from Gromeka-Lamb form of Navier-Stokes equations where the vorticity and velocity are known from solution of (2.2)–(2.3). The pressure is calculated by integrating Gromeka-Lamb equations along the different paths [22, 23]. Pressure must not be dependent on the integration path.

The computational algorithm is detailed in [8, 9, 23]. The pseudo-spectral direct method is employed for solution of Eq. (2.2); the ADI method is used for (2.3). The two-parameter approximation is used for calculation of boundary vorticity  $\Omega_s$ , which simultaneously serves as the boundary condition for Eq. (2.3) solved separately. The novel stage of computational algorithm deals with the correction of the vorticity field. This correction, in the first place, recovers the vorticity in the wake where the vorticity dissipation takes place on the coarse mesh, and, in the second place, introduces the pressure compatibility condition explicitly into the calculation of vorticity on the airfoil surface, and further into the boundary condition for Eq. (2.3).

A complete description of the method is given in [23] and the correction stage is derived in [24].

### 3. Results of computation

The “O-type” orthogonal curvilinear computational mesh is used with 128 mesh nodes in the  $\eta$  direction (along an airfoil surface), and with 80 mesh nodes in the  $\xi$  direction (from an airfoil surface to the outer boundary of computational region which is nearly the circle of radius equal to ten airfoil chord lengths). The additional compression in the  $\xi$  direction is employed [3, 23]. The minimum mesh sizes at the TE are  $h_n = 3.529 \times 10^{-5}$ ,  $h_\tau = 9.009 \times 10^{-4}$ , and at the LE are  $h_n = 71.343 \times 10^{-4}$ ,  $h_\tau = 3.955 \times 10^{-3}$ , where  $n$  and  $\tau$  are the indices of normal and tangential directions.

The relative characteristics discussed below are obtained as the difference of these characteristics at the time instant  $t$  from those at the time  $t + \Delta t$  where  $\Delta t = 0.1$ . Dependence of the discussed phenomenon (at least, its characteristics shown in the fields of relative velocity components and vorticity) on  $\Delta t$  may

be rather high. This is the same problem as a dependence of turbulent flow characteristics on the interval taken for averaging. Nevertheless, the previous study of viscous flow around a NACA0012 airfoil ([3, 7]) shows that the integral characteristics (the lift and drag coefficients) oscillate with a period equal to 0.1 – 0.2. These oscillations are related to generation of vortex spots near TE ([10]) (the momentum spots). These results had been obtained at different time steps in computational algorithms. The present results were computed with  $dt = 0.00125 - 0.0025$ . The time increment  $\Delta t = 0.1$  used for relative fields shown in Figs. 2 through 7 is chosen because this is a basic period of TE spot generation (at least for  $Re = 10000$ ).

In Figs. 1a through 1f the flow around airfoil NACA0012 at  $Re = 1000$  and angle of attack of  $5^\circ$  is represented by the lines of equal values of relative  $V_\xi$  velocity component drawn for successive time moments with the interval  $\Delta t = 0.1$ . Disturbances in Fig. 1 can be characterized as the “dispersion impulse”, which gives rise to the complex wave disturbances. The lines of equal values of relative  $V_\eta$  velocity components are in Fig. 1g, and in Fig. 1h the relative vorticity is presented. Disturbances of  $V_\xi$  and  $V_\eta$  are small, but the disturbances of vorticity are great and have the maximum on the airfoil surface where the velocity is zero. The outer boundary of the vortex layer is the second region of possible strong vorticity perturbation, see [17]. The vortex structures in the wake flow in Fig. 1h have the opposite signs.

At  $Re = 10000$  the disturbances in the boundary layer most clearly look like mainly the vortex disturbances. Figure 2 depicts the lines of equal values of the relative  $V_\xi$  velocity component; Fig. 3, the same ones for relative  $V_\eta$  velocity component; and Fig. 4, lines for relative vorticity. Disturbances of  $V_\xi$  and  $V_\eta$  are small again: in Figs. 2 and 3, zeroes of these relative quantities take place within the boundary layer, whereas in the wake, only the lines with values  $k \times 0.0125$ , ( $k = 1, 2, \dots, 5$ ) of these quantities are revealed. We see that the vorticity disturbances look like the usual  $\lambda$ -structure of the boundary layer, see also [7, 9], and have the maximum on the airfoil surface. We can assert that the greatest disturbances are spread over the airfoil surface and form a vortex wave (note that the velocity at the surface is zero). Hence, it becomes clearly that the strong interaction of a surface vortex wave with the physical fields (such as pressure and temperature) around the flow separation point and in the vicinity of the trailing edge is the decisive phenomenon in the flow around an airfoil. In principle, we can say about analogy with streaming/shedding waves (see [25]) which here assume the form of shedding waves of vorticity (the surface tension waves). Again, the vortex structures in the wake flow in Fig. 4 have opposite signs.

The primary development of vorticity waves is clearly shown in the case of the flow at  $Re = 30000$  also. Figure 5 demonstrates the lines of equal values of relative  $V_\xi$  components; Fig. 6, relative  $V_\eta$  components; and Fig. 7, relative vorti-

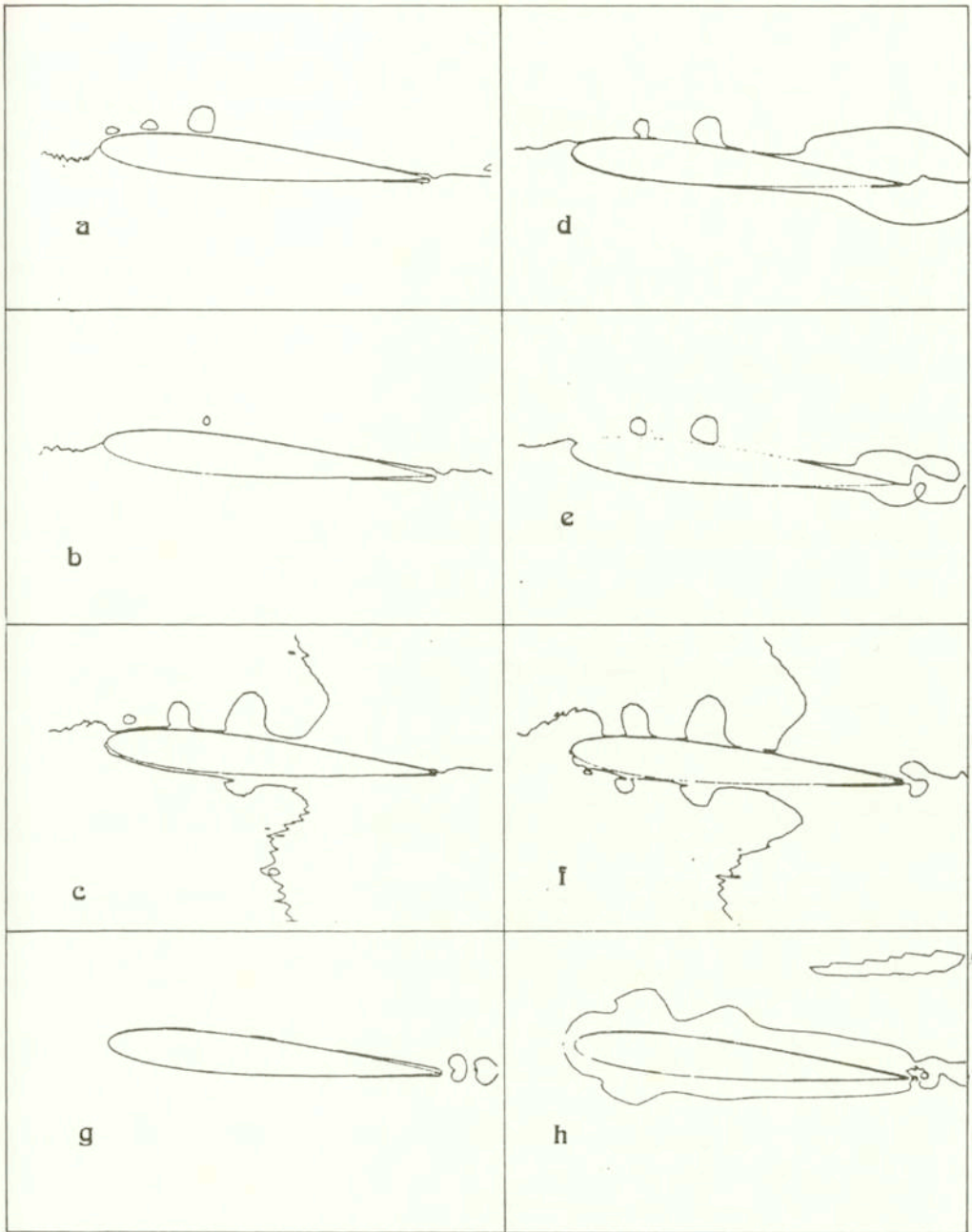


FIG. 1. The lines of equal values ( $\bar{V}_\xi = (k-1) \times 0.0125 - 0.1375$ ,  $k = 1, 2, \dots, 5$ ) of relative  $\bar{V}_\xi$  component of velocity (a-f), relative  $\bar{V}_\eta$  component of velocity (g) around NACA0012 airfoil at  $Re = 1000$  and angle of attack of  $5^\circ$ . The lines of equal values of relative vorticity (h) for the values  $\Omega_i = (i-1) \cdot 0.25$ ,  $i = 1, \dots, 11$ ;  $\Omega_k = (k-1) \times 20 - 50$ ,  $k = 1, 2, 3$ ;  $\Omega_m = (m-1) \times 0.25$ ,  $m = 1, \dots, 11$ ;  $\Omega_n = 20 \times n$ ,  $n = 1, 2, 3$ . Note that (g) and (h) correspond to the time instants of (f).

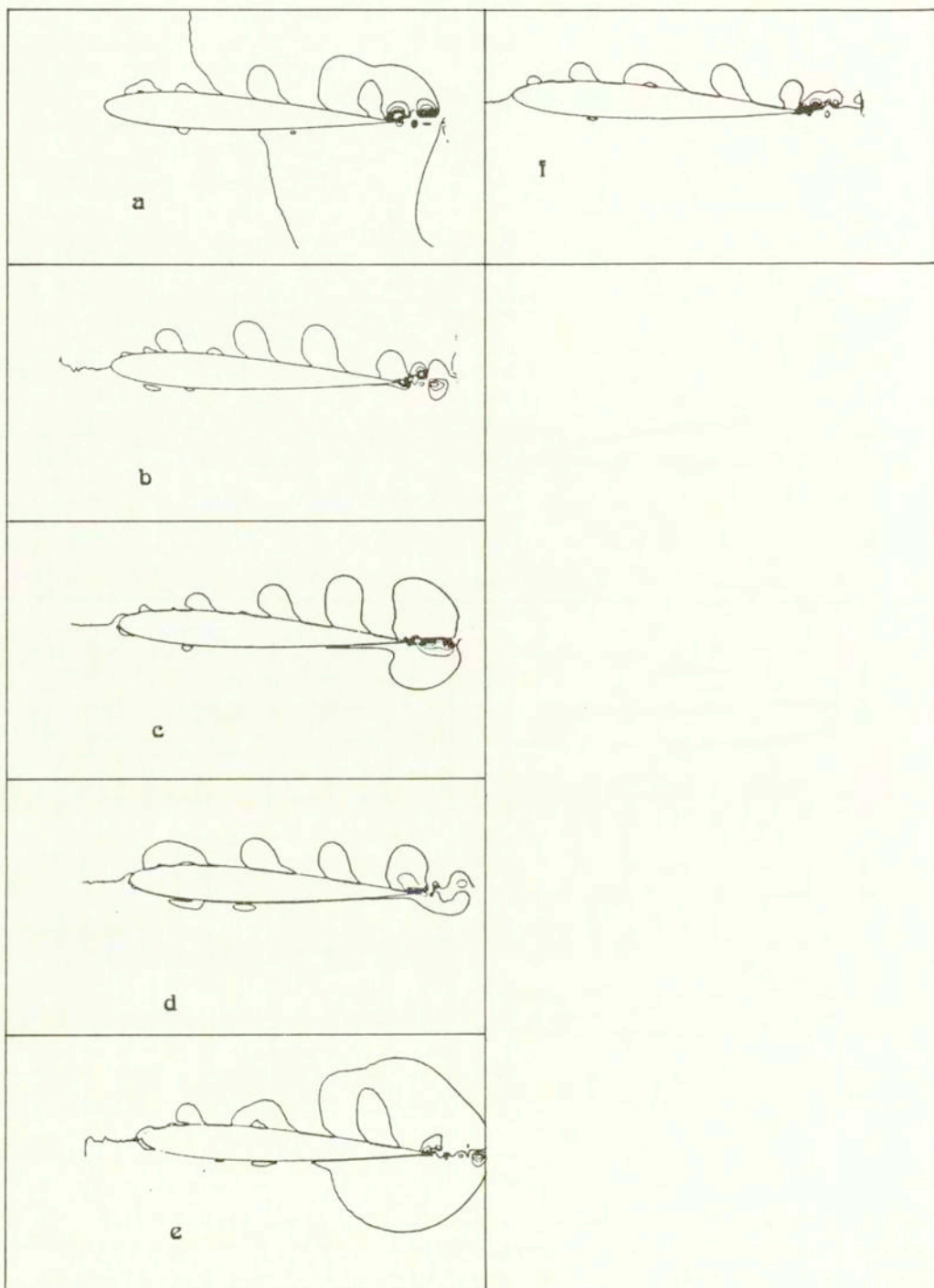


FIG. 2. The lines of equal values (which correspond to Fig. 1) of relative  $\bar{V}_\xi$  component of velocity (a-f) around NACA0012 airfoil at  $Re = 10\,000$  and angle of attack of  $5^\circ$ .



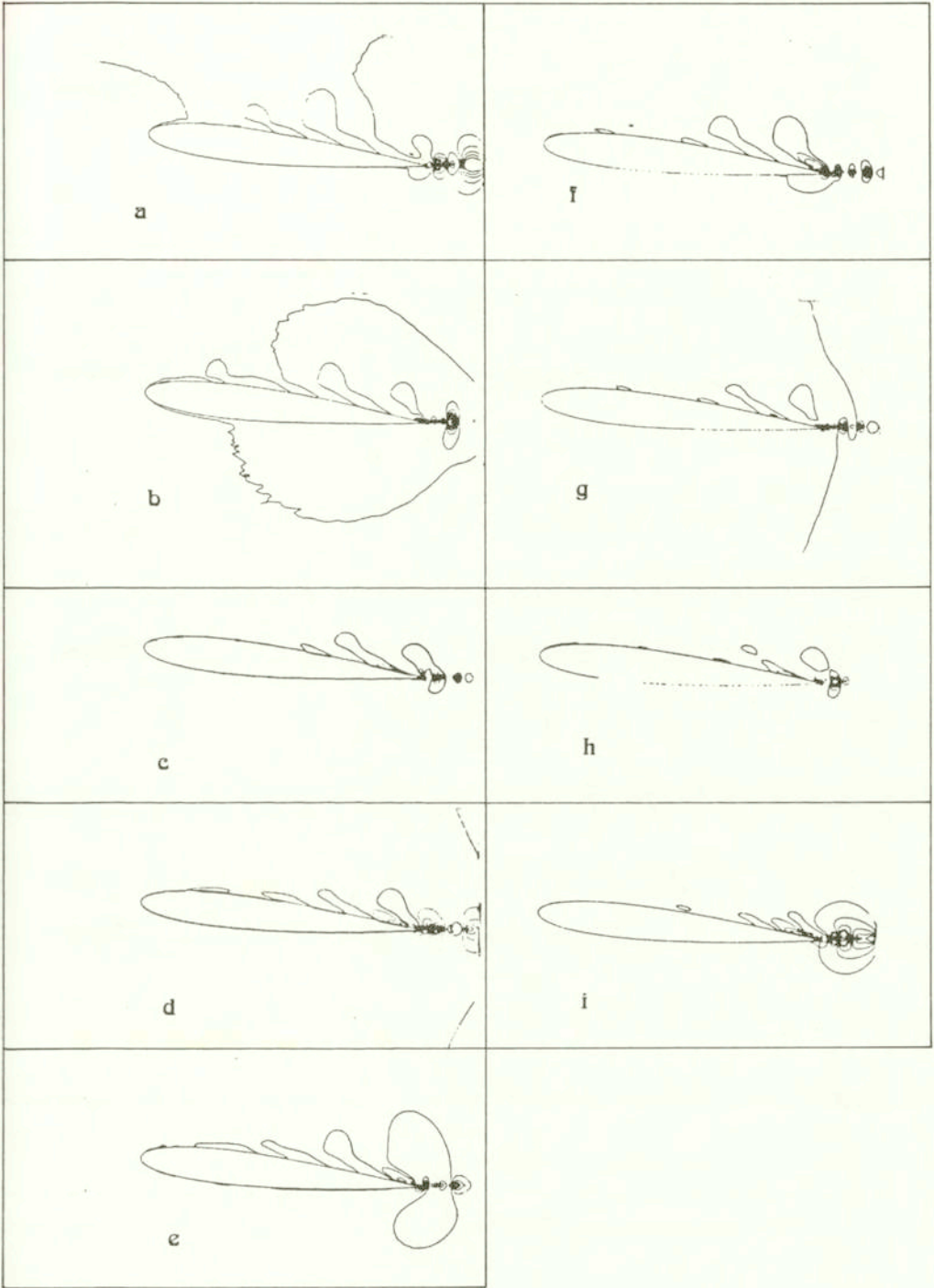


FIG. 3. The lines of equal values (which correspond to Fig. 1) of relative  $\bar{V}_n$  component of velocity (a-i) around NACA0012 airfoil at  $Re = 10\,000$  and angle of attack of  $5^\circ$ .

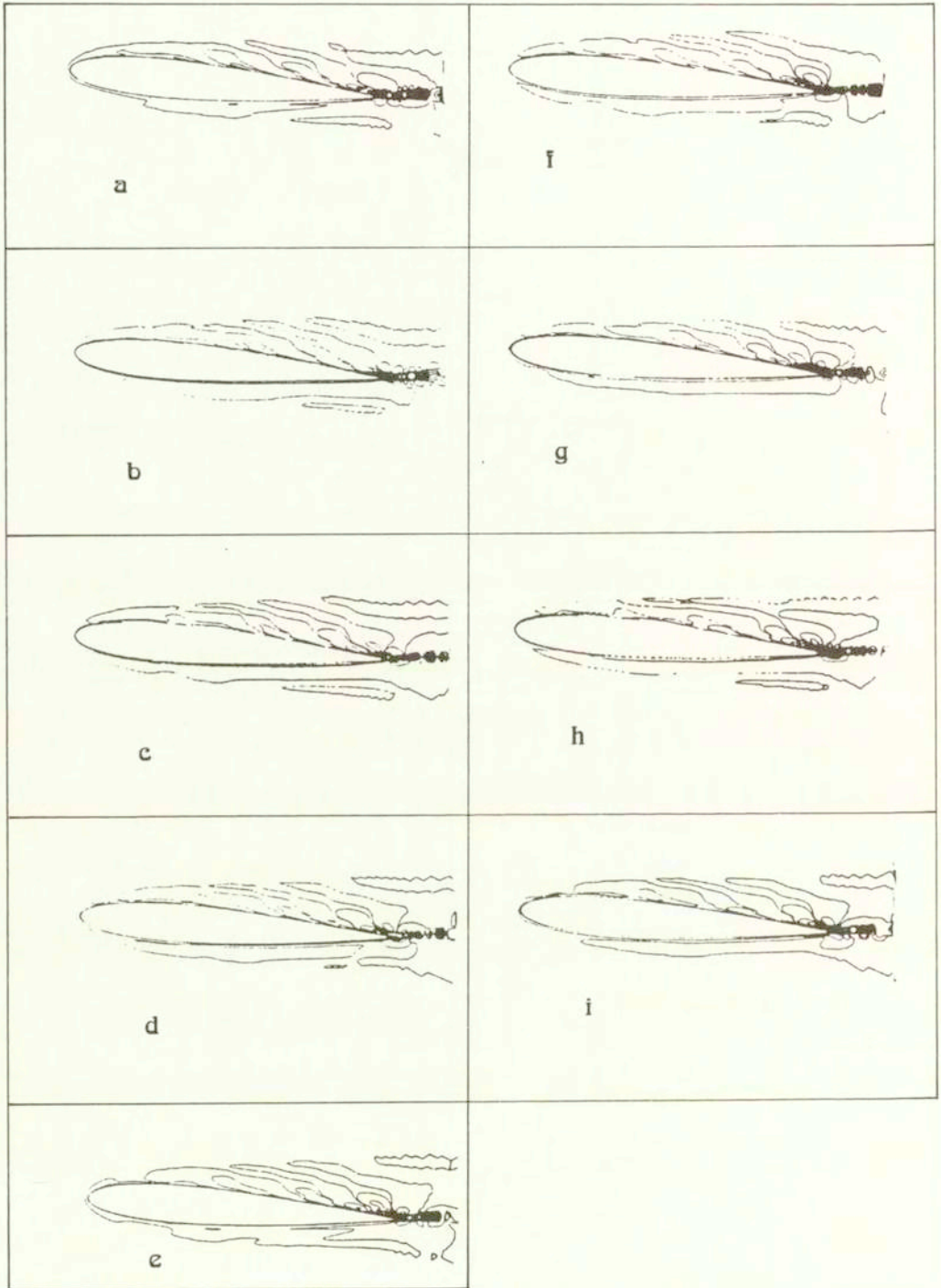


FIG. 4. The lines of equal values (which correspond to Fig. 1) of relative vorticity (a-i) around NACA0012 airfoil at  $Re = 10\,000$  and angle of attack equal to  $5^\circ$ .

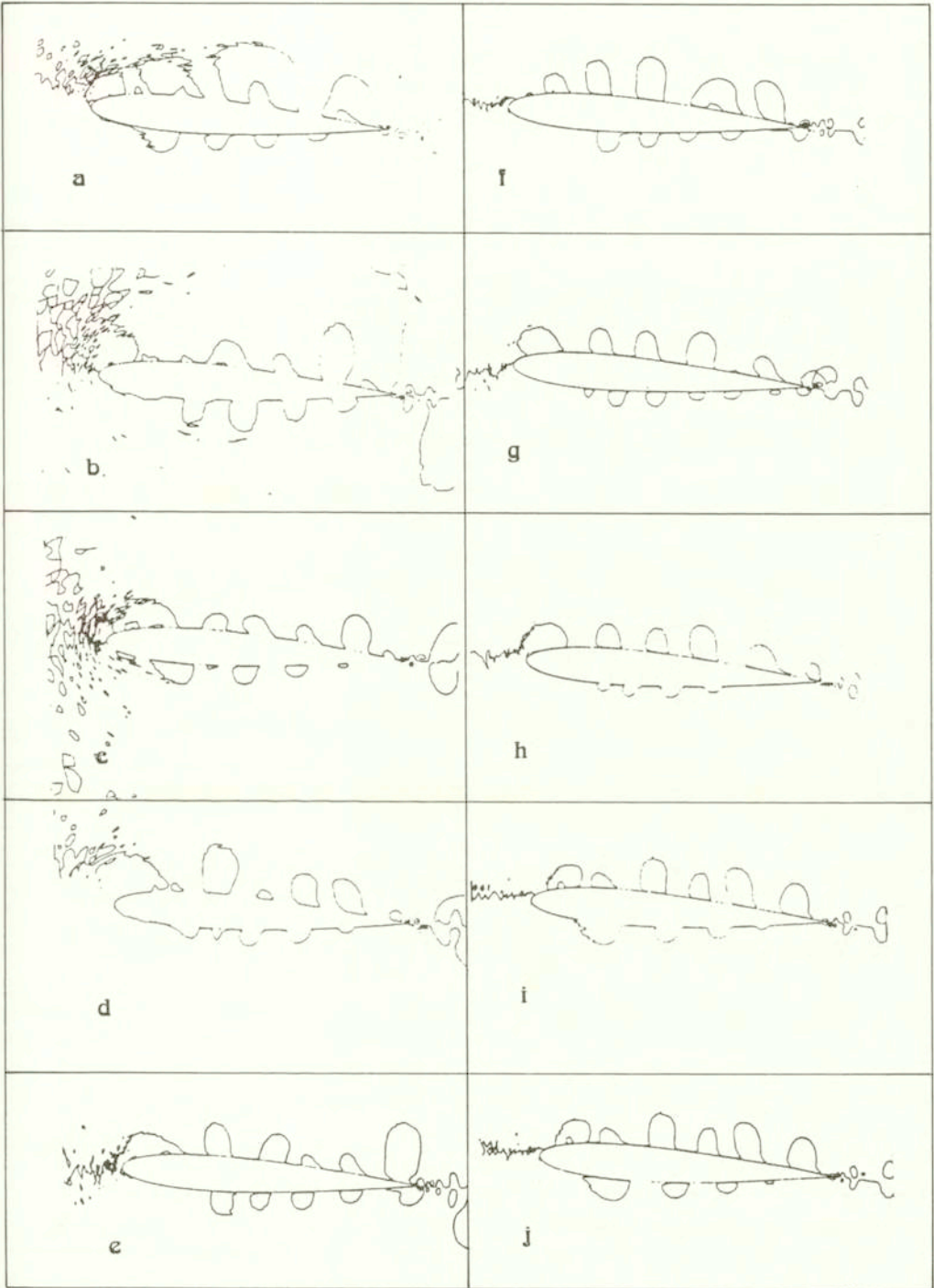


FIG. 5. The lines of equal values (which correspond to Fig. 1) of relative  $\bar{V}_\xi$  component of velocity (a-k) around NACA0012 airfoil at  $Re$  30 000 and angle of attack equal to  $5^\circ$ .

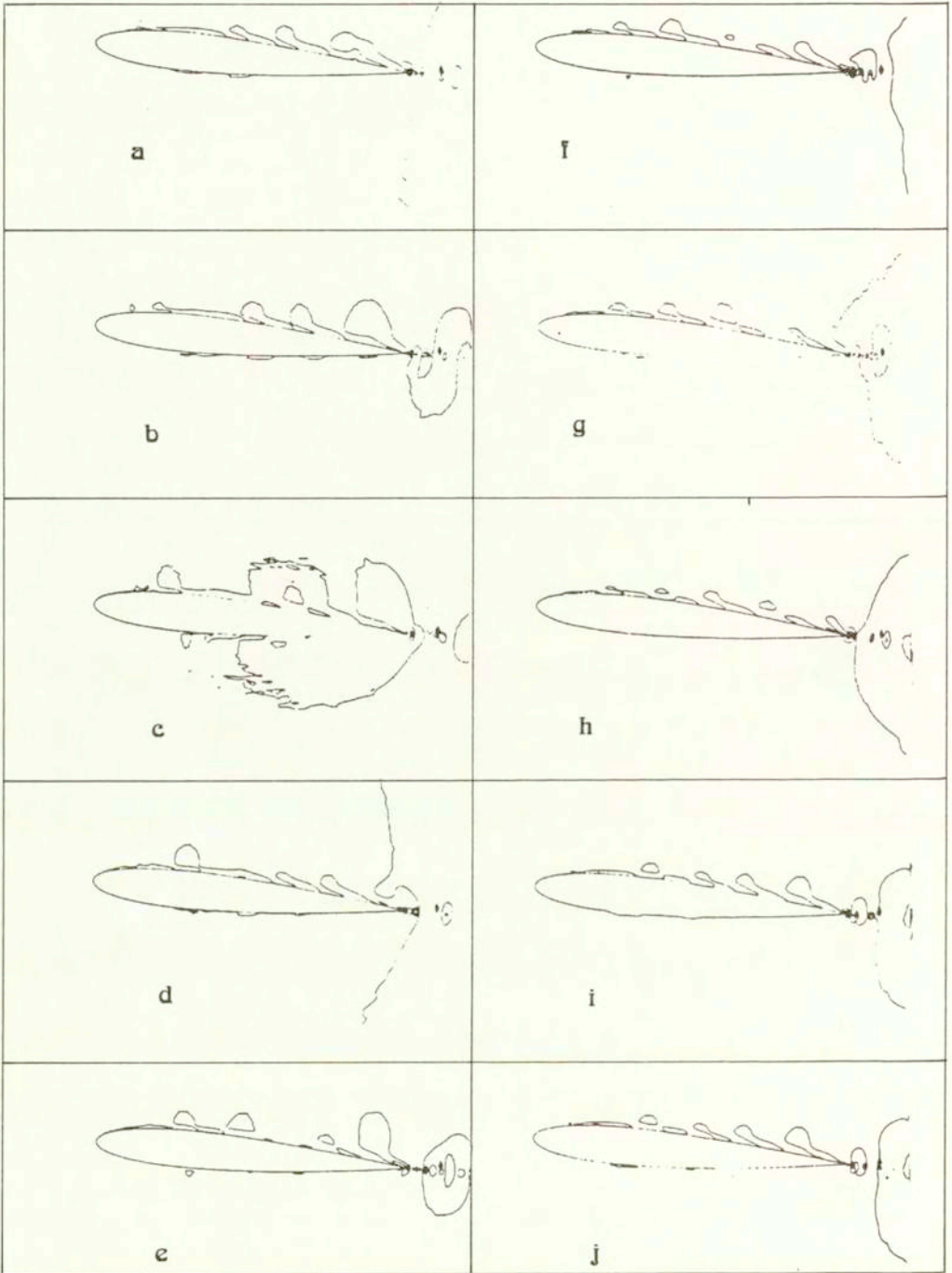


FIG. 6. The lines of equal values (which correspond to Fig. 1) of relative  $\bar{V}_n$  component of velocity (a-k) around NACA0012 airfoil at  $Re= 30\,000$  and angle of attack equal to  $5^\circ$ .

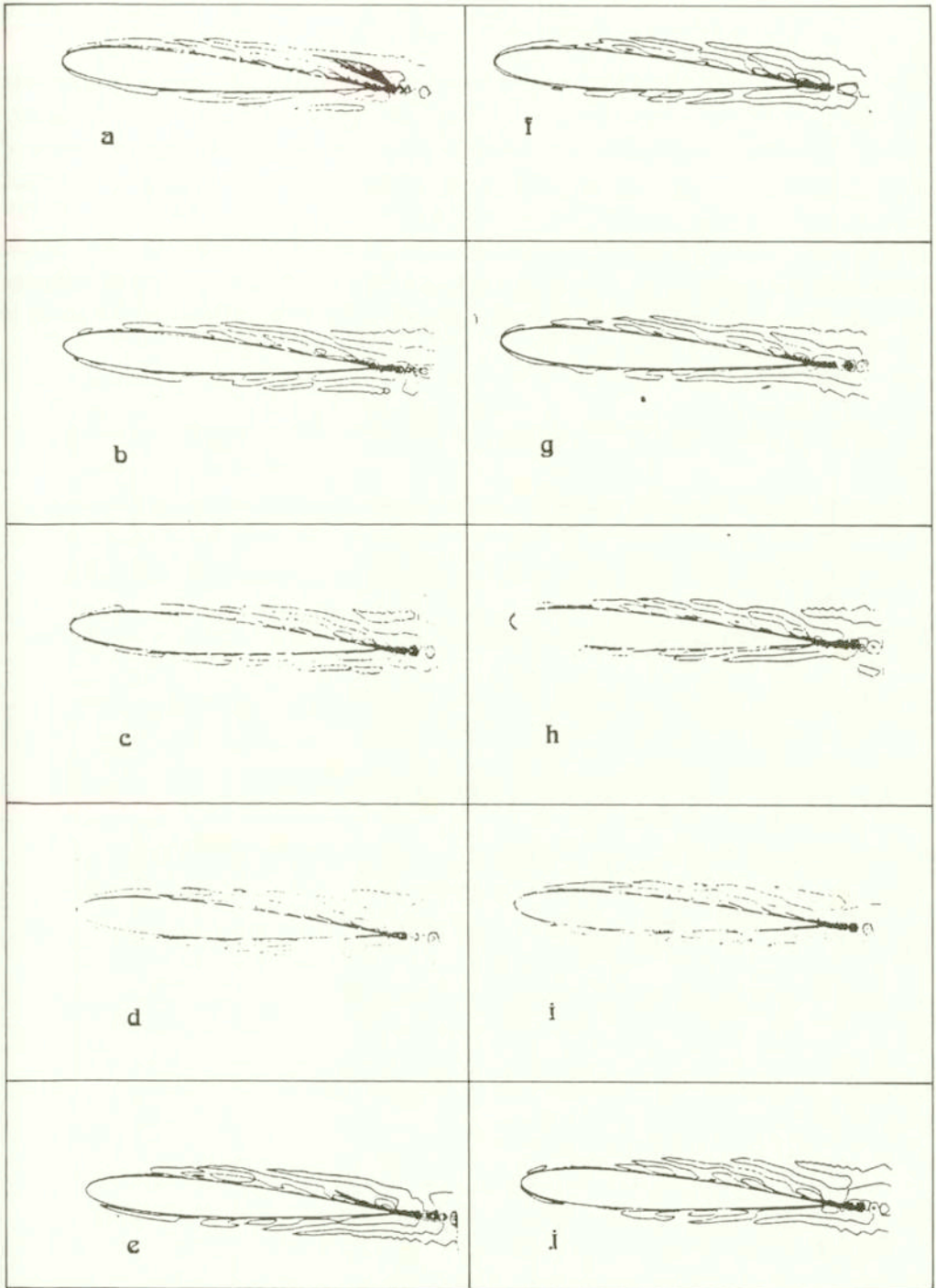


FIG. 7. The lines of equal values (which correspond to Fig. 1) of relative vorticity (a-k) around NACA0012 airfoil at  $Re = 30\,000$  and angle of attack of  $5^\circ$ .

city (the vortex structures in the wake have opposite signs). We can note also that the intensity of surface vorticity waves (i.e., the surface tension waves) is closely related to a corresponding pressure disturbance. Simultaneously, the existence of strong vortex-pressure transition in the vicinity of TE is confirmed by the fact that the pressure at the trailing edge in the Fig. 8 obtained for  $Re = 10000$ ,  $\alpha = 5^\circ$ ,  $\Gamma = -0.21$  and  $Dy = 4$  (where  $Dy$  is the intensity of the first dipole term with the axis directed along the vertical axis  $Oy$  in asymptotics of velocity at a far boundary, see [3], and  $\Gamma$  is intensity of circulation in the asymptotics) is

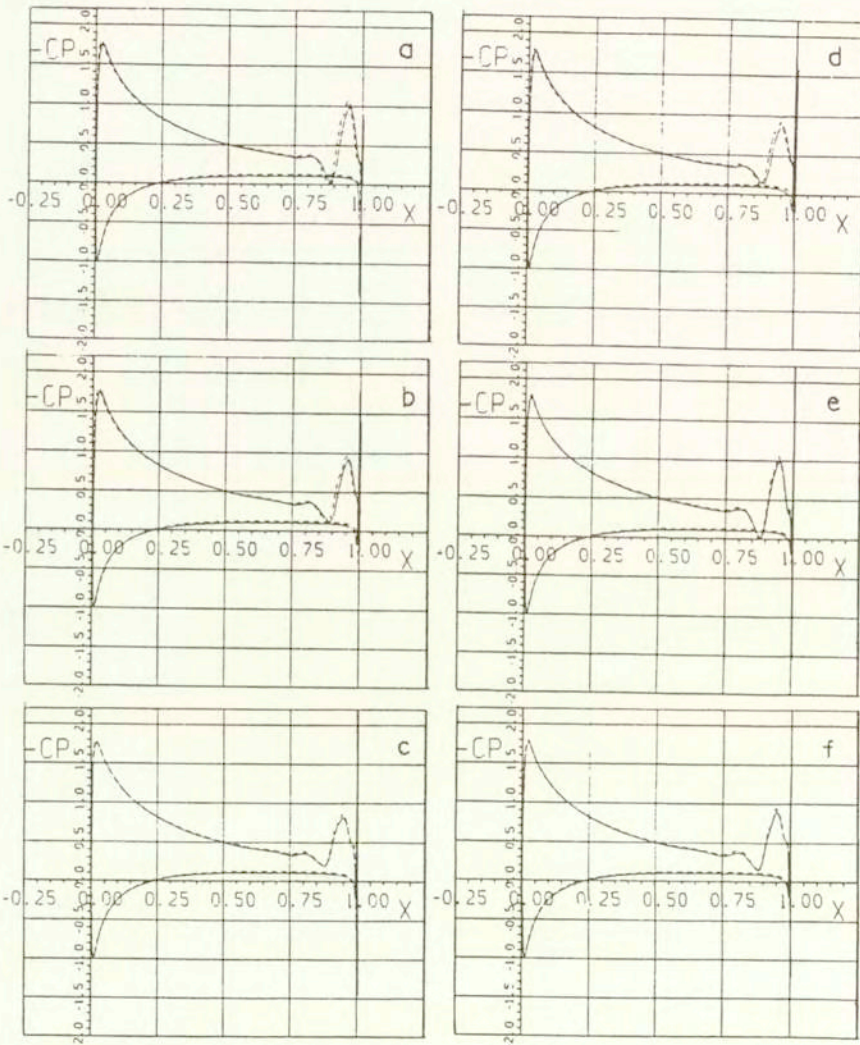


FIG. 8. The pressure coefficient distribution around NACA0012 airfoil at  $Re = 10000$  and angle of attack equal to  $5^\circ$  (a-f) correspond to successive time instants with interval  $\Delta t = 0.1$ .

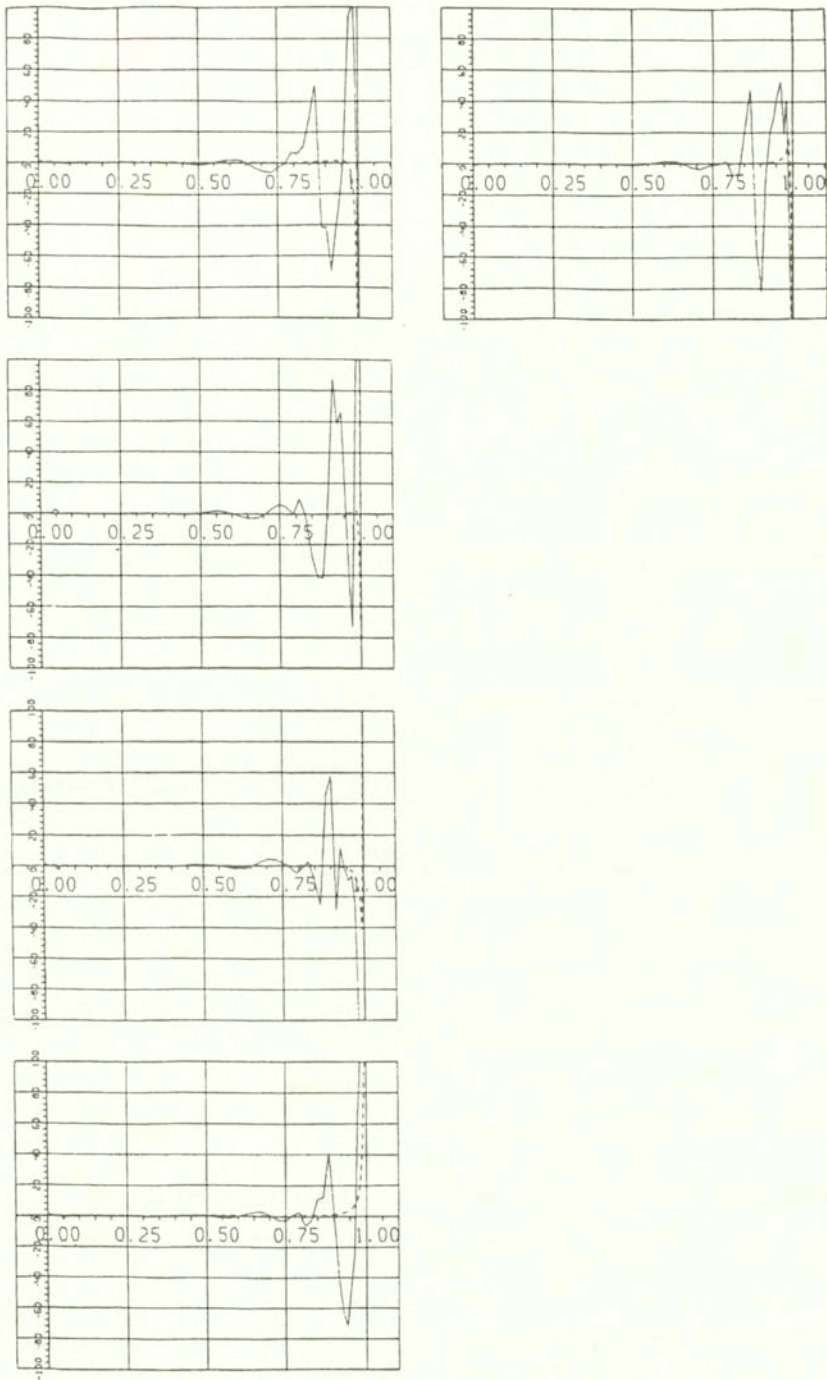


FIG. 9. The surface relative vorticity distribution along the airfoil NACA0012 at  $Re = 10\,000$  and angle of attack equal to  $5^\circ$ . The solid line corresponds to the upper part and dotted line to the lower part of an airfoil surface. Time increment equals 0.1.

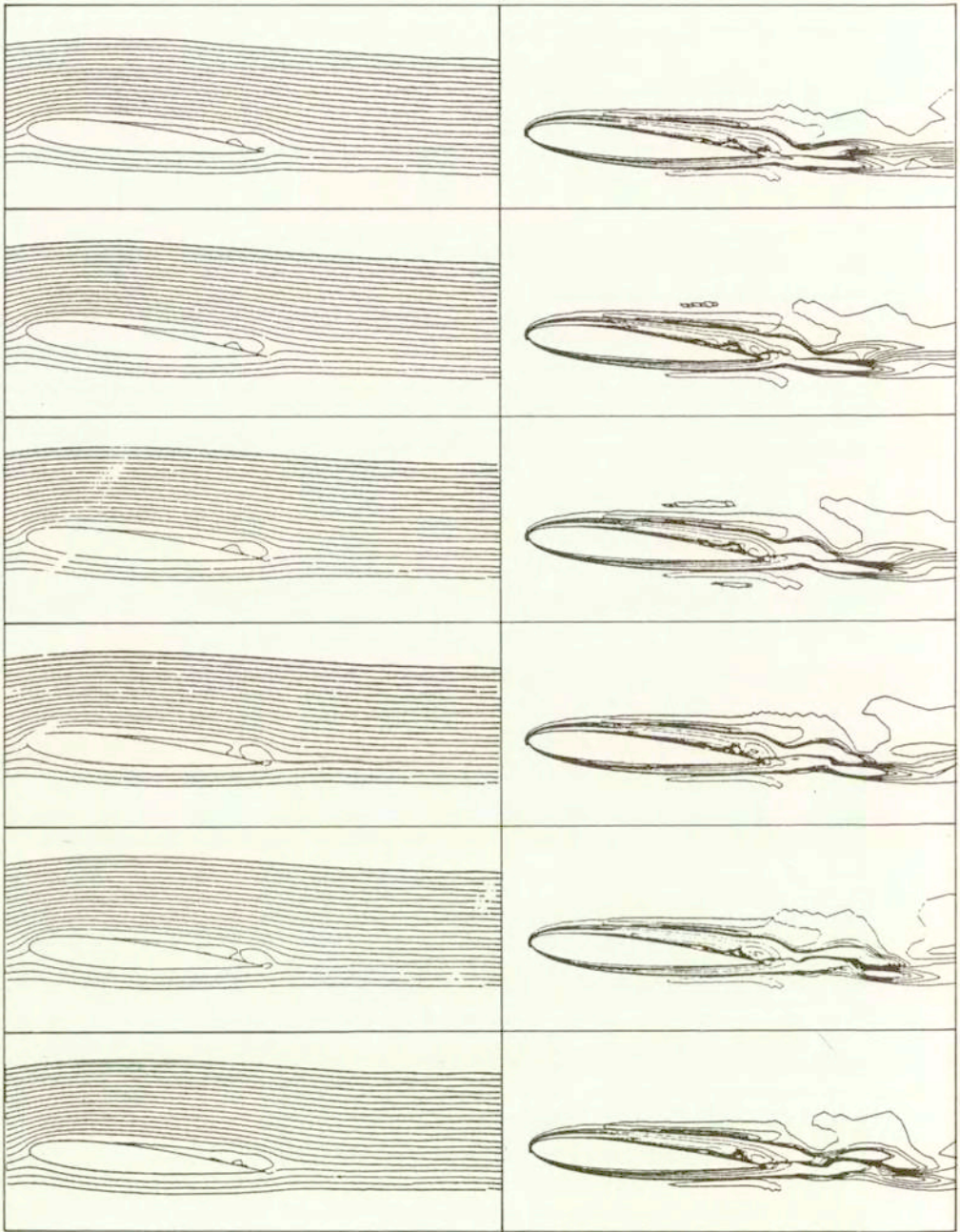


FIG. 10. Streamlines (a-f) and equal vorticity lines (g-m) around NACA0012 airfoil at  $Re = 10000$  and angle of attack equal to  $5^\circ$ . (a-f), (g-m) correspond to successive time instants with interval  $\Delta t = 0.1$  (they coincide with the time instants of Fig. 8). The values of  $\psi$  are  $\psi_i = (i - 1) \times 0.025 - 0.075$ ,  $i = 1, \dots, 22$ ; the values of vorticity:  $\Omega_k = (k - 1) \times 0.25 - 1.25$ ,  $k = 1, \dots, 5$ ;  $\Omega_l = (l - 1) \times 20 - 50$ ,  $l = 1, 2, 3$ ;  $\Omega_m = (m - 1) \times 0.25$ ,  $m = 1, \dots, 5$ ;  $\Omega_n = (n - 1) \times 20 + 10$ ,  $n = 1, 2, 3$ .



greater than pressure at the stagnation point (the solid lines corresponds to pressure obtained by integration of Gromeka – Lamb equation from  $s_\infty$  to  $s$ , and dotted line corresponds to the pressure obtained by integration over the airfoil surface). This is the case of pressure impulse formation. The coincidence of pressure over an airfoil obtained by integration along two different paths confirms that the solution is accurate. The surface (relative) vorticity waves are presented in Fig. 9. Streamlines for this flow are depicted in Fig. 10. The results in Figs. 8 – 10 confirm that unsteady TE flow described in [7, 9, 10] is not related to pressure imbalance which had been observed in these earlier calculations.

Streamlines and equal vorticity lines for the viscous flow around NACA0012 airfoil at  $Re = 10\,000$  are presented in [3, 7–9, 12, 16, 17] and at  $Re = 100\,000$  in [16].

#### 4. Discussion

We must underline that the problem of vortex dipole stability is a very complex problem of mathematical physics. Simultaneously, some phenomena which can only be studied by direct numerical simulation take the lead in this process. Flow separation on the airfoil and in vicinity of the trailing edge impose disturbing action on the vortex dipoles (at TE and LE). As the result, the surface vorticity waves running over the airfoil surface from LE to TE are derived, see Fig. 9. These waves are intensified at the flow separation point and, essentially, in the vicinity of TE. Two vortex waves run into each other at TE and the complex vortex-acoustic-heat interaction characterizes this collision. Accumulation of disturbances provokes generation of vortex spots [9, 10]. The shedding of vortex spots from TE imposed again disturbance of the vortex dipole at LE. This process has the known theoretical basis described below.

Generation of vortex spot in vicinity of TE reveals generation of vorticity of a certain sign in the boundary layer. An equal portion of vorticity of opposite sign must be generated in the flow due to the total vorticity conservation law. The airfoil surface (especially around LE) is the generator of vorticity (note that vorticity can also be generated in critical layers [23]). We repeat here that the vortex spot is intermediate between a vortex and a vortex wave. The corresponding vortex spot (with vorticity of opposite sign to the vortex spot at TE) near LE is difficult to appear as a consequence of the LE spot instability. For this reason, vortex spot formation at TE provokes the complex perturbations at LE. Some of these perturbations are realized as surface vorticity waves, and other ones – as a pressure perturbation and upstream perturbation of potential flow which thereafter run onto the airfoil. We cannot exclude the appearance of local anisotropic flow at LE because the transition of essential vorticity perturbation into disturbances of upstream potential flow (or generation of

vortex spots in upcoming flow) is a quite complex phenomenon. This is the reason for generation of dispersion impulse in the flow. Thus, the perturbations of dipole reveal self-induction, and we have the analogy with self-induced flow separation ([26]).

The difficulties in theoretical description of dipole bifurcation consist in a special initial phase of this phenomenon which is characterized by emission of disturbances in a microwave part of the wave spectrum (this is revealed by perturbation of line  $\{V_\xi = 0\}$  running on to the airfoil LE, see Figs. 1 through 3). But the final stage of dipole bifurcation takes place in the short- and long-wave disturbances in the boundary layer. The transition from microwave disturbances to the short-wave ones is accompanied by dispersion. This is the reason why we choose such characteristic as "dispersion impulse" for the wave process in the Fig. 1. But the phenomenon as a whole, of course, is well defined by the notion of "dipole bifurcation". Note again that the last conclusion is based on a qualitative coincidence of zero streamlines behavior in the vicinity of TE (this kind of behavior is detailed in [7, 9]) with the one presented in [14] theoretically describing dipole bifurcation. We must emphasize that there is a theoretical problem on the smallest scale for incompressible viscous flow ([27]). This problem is inherent in dipole bifurcation phenomenon.

The complexity of numerical simulation of this phenomenon by finite-difference methods is connected with the fact that the minimum length of the waves which are correctly described by computational models of continuum media is equal to the mesh step. The dipole bifurcation process features microwaves whose wavelengths are smaller than the mesh step. This may be the main reason of dispersion impulse in solution of N-S equations by finite-difference algorithms. But we do not have to reject the possibility of there being real physical foundations for the phenomenon. Undoubtedly, any complication of the rheology law at initial turbulence leads to inclusion of dispersion and energy dissipation terms in N-S equations ([21, 28]) which thereafter will describe the vortex erosion effects, bursting, dispersion impulse, soliton-like structures, see [12, 13]. This idea is close to consideration of some oscillating solutions (wiggles) proposed by GRESHO *et al.* [29].

We must formulate conclusion for the numerical solution and can suppose for theoretical one that the vortex/vorticity disturbances and the surface vorticity waves are the main physical factor absorbing the dispersion impulse perturbation. In such a way, the dipole bifurcation near LE can give rise to complex perturbation which we can consider as a novel type of vortex-wave perturbations. The latter are different from the Tollmien-Schlichting waves, Rayleigh waves. But after interaction with LE, this vortex-wave perturbation transforms into the Tollmien-Schlichting waves, Rayleigh waves and vortex waves. Thereby, all types of disturbances are generated and each of these is realized in the region containing

the most suitable conditions for this kind of waves. Note that the disturbances around LE facilitates the development of critical layers.

The results obtained by the conventional computational scheme described in [23] with these obtained by predictor-corrector scheme [24] were compared to show that the pressure impulse at TE and the dispersion impulse at LE are closely related. Fulfillment of the pressure compatibility condition in computations reduces the dispersion impulse at LE and increases the pressure impulse at the TE. But the dispersion impulse at LE is conserved and we can expect that its significance increases with taking into account the heat and compressibility effects.

If we consider such complex phenomenon as a strong dipole hysteresis [30] then we find the direct analogy with the dipole bifurcation perturbations which in this case are provoked by external dipole. The great pressure gradient is derived at the TE in the case of a strong dipole hysteresis. Then, vorticity waves on the upper surface cannot leave TE, and the corresponding pressure impulse increases the region of flow separation at initial stage of hysteresis. Thereafter the vortex disturbances in the separation region are growing and the spread separation develops as a consequence of vorticity accumulation.

Finally we must note that, in order to take into account the dependence of minimum wavelength on the mesh steps, it is necessary to investigate the frequency of dipole bifurcation (for example, at  $Re = 10\,000$  from the computational model parameters. The more comprehensive research requires parametric approximation of nonlinear terms in Eq. (2.3) as proposed (and implemented) in [12, 13] for the problem is under study.

### Acknowledgement

This paper had been presented at the 5th International Conference "Aircraft and Helicopters' Diagnostics (AIRDIAG'97)" Warsaw, December 11–12, 1997.

### References

1. G. A. OSSWALD, K. N. GHIA and U. GHIA, *Analysis of potential and viscous flows past general two-dimensional bodies with arbitrary trailing edge geometries*, AIAA 89-1969-CP.
2. K. N. GHIA, G. A. OSSWALD and U. GHIA, *Simulation of self-induced unsteady motion in the wake of a Joukowski airfoil*, Supercomputers and Fluids Dynamics, Lecture Notes in Engineering, 24, C. A. BREBBIA and S. A. ORSZAG [Eds.], 118–132, Springer-Verlag, Berlin 1986.
3. M. N. ZAKHARENKOV, *Far field boundary conditions in a viscous incompressible flow past an airfoil* [in Russian], *Matem. modelirovanie*, 2, 3–18, 1990. (Mathematical Simulation, 1990).

4. J. Z. WU and J. M. WU, *Interaction between a solid surface and a flow field*, [in:] J. Fluid Mechanics, 1994.
5. MENG WANG, K. SANJIVA, K. LELE and M. PARVIZ, *Computation of quadropole noise using acoustic analogy*, AIAA Journal, **34**, 11, 2247-2254, November 1996.
6. Y. LECOINTE, J. PIQUET, *Unsteady viscous flow round moving circular cylinders and airfoils*, AIAA 7th Computational Fluid Dynamic conference. Cincinnati, Ohio, July 15-17 1985, Collection of Technical Papers. New York, AIAA CP 85-1490.
7. M. N. ZAKHARENKO, *The development of a nonstationary separation and coherent structures in a two-dimensional viscous incompressible flow around a body*, Arch. Mech., **48**, 2, 395-410, 1996.
8. M. N. ZAKHARENKO, *Airfoil lift simulation in a viscous flow*, [in Russian], Preprint TsAGI **70**, p. 27, 1993.
9. M. N. ZAKHARENKO, *Small-scale vortex structures in numerical solutions of two-dimensional Navier-Stokes equations* [in Russian, contains the translation into English], Preprint TsAGI **69**, p. 58, 1993.
10. M. N. ZAKHARENKO, *Generation of vortices and vortex spots - spots of momentum losses, in the viscous flow around an airfoil* [in Russian], [in:] Scientific Papers of International Symposium on Ship Hydrodynamics devoted to 85th anniversary of birthday of A.M. Basin, 450-470, St Peterburg 1995.
11. Yu. J. SHOKIN, N. N. YANENKO, *Differential approximation method. Application to gas-dynamics* [in Russian], Nauka, Novosibirsk, Sib. branch of Academy of Sciences of USSR, 1985.
12. M. N. ZAKHARENKO, *Computation of bifurcating viscous flow around circular cylinder performing rotational oscillation in uniform flow*, [in:] Proceedings of the 2nd European Nonlinear Oscillations Conference. [Eds.] L. PUST and F. PETERKA, **2**, September 9-13, Prague, 249-254, 1996.
13. M. N. ZAKHARENKO, *Hydrophysical effects in the viscous incompressible flow around a circular cylinder*, Proceedings of Third Intern. Conf. on New Energy Systems and Conversions, G. L. DEGTYAREV and V. S. TERESHCHUK [Eds.], September 8-13, 197-202, Kazan 1997.
14. V. S. SADOVSKY, G. I. TAGANOV, *On discrete behaviour of vortex generation at initiation of circulating flow around the airfoils* [in Russian], PMTF, **4**, 44-48, 1988.
15. M. N. ZAKHARENKO, N. I. MIKHAYLOVA, *Vortex structures in the oscillating body wake and fixed body wake* [in Russian], [in:] Turbulent flows and experimental technique, Theses of papers of VI All-Union (USSR) Congress on theoretical and practical aspects of turbulent flows, Ju R. RUDY [Ed.], 110-112, Tallin, 1989.
16. M. N. ZAKHARENKO, *Influence of flow lamination and detached separation on laminar-turbulent transition and turbulence structure*, Ninth Int. Symp. on Transport Phenomena (ISTP-9), 25-28 June, 1996, Singapore, S. H. WINOTO, Y. T. CHEW and N. E. WIJEYSUNDERA [Eds.], **2**, 1268-1274, 1996.
17. M. N. ZAKHARENKO, *Numerical simulation of hysteresis transformations of vortex flow near an airfoil*, Thermophysics and Aeromechanics, **4**, 1, 25-31, 1997.
18. M. E. GOLDSTEIN, *The role of nonlinear critical layers in transition to turbulence in boundary layers*, 1st AIAA Theoret. Fluid Mech. Meeting. June 17-20, 1996 New Orleans, La., AIAA 96-2132.

19. X. WU, *On oblique-mode breakdown of boundary layers*, 1st AIAA Theoret. Fluid Mech. Meeting, June 17-20, 1996 New Orleans, LA, AIAA 96-2133.
20. O. S. RYSHOV, E. D. TERENTIEV, *Vortex spots in the boundary layer*, Fluid Dyn. Trans, Polish Scientific Publishers, **13**, 203-234, Warsaw 1987.
21. L. I. SEDOV *On perspective directions and problems in mechanics of continuum* [in Russian], PMM, **40**, 6, 963-980, 1976.
22. M. N. ZAKHARENKOV, *Singularities of finite-difference scheme for two-dimensional N-S equation solution, connected with the boundary conditions statement on a solid surface* [in Russian], ZhVMM (Zhurnal Vychislitel'noy Matematiki i Matematicheskoy Fiziki), **30**, 8, 1224-1236, 1990; Preprint TsAGI No. 1, p. 22, Moscow, 1989.
23. M. N. ZAKHARENKOV, *Unsteady detached separation from a circular cylinder performing rotational oscillation in a uniform viscous incompressible flow*, Intern. J. for Numer. Meth. in Fluids, **25**, 125-142, 1997.
24. M. N. ZAKHARENKOV, *On the pressure uniqueness in solution of Navier-Stokes equations written in the terms of stream function and vorticity* [in Russian], Matemat. Modelirovanie, **1**, 3-10, 1998.
25. A. GUBANOV, *The Rayleigh waves on the rigid-liquid boundary* [in Russian], ZhETF (J. Experimental and Theoretical Physics), **15**, 497, 1945.
26. K. STEWARTSON, P. G. WILLIAMS, *Self-induced separation*, Proc. Roy. Soc. London. Ser. A, **312**, 1509, 181-206, 1969.
27. W. D. HENSHAW, H. O. KREISS and L. G. REYNA, *On the smallest scale for the incompressible Navier-Stokes equations*, Theoretical and Computational Fluid Dynamics, **1**, 65-95, 1989.
28. N. S. KOKOSHINSKAYA, *On the system of equation describing viscous fluid over a wide range of Reynolds number* [in Russian], In Mathematical Models for Natural Sciences. Moscow State University, 17-26, 1995.
29. P. M. GRESHO, R. L. LEE, *Don't suppress the wiggles - they're telling you something*, Computers and Fluids, **9**, 223-253, 1981.
30. M. N. ZAKHARENKOV, *Simulation of airfoil aerodynamic hysteresis for flight safety problems*, 4th International Conference on Aircraft and Helicopters Diagnostics (AIRDIAG'95), 6-7 December, Warsaw 1995, Informator ITWL 338/96, Warsaw, 1996.

CENTRAL AERO-HYDRODYNAMIC INSTITUTE  
140160 Zhukovsky, Moscow region, Russia

Received December 12, 1997, new version July 3, 1998.